ELSEVIER

Catalysis Today 64 (2001) 69–81

CATALYSIS TODAY

www.elsevier.com/locate/cattod

A comparative study of the oxidation of CO and CH_4 over $Au/MO_x/Al_2O_3$ catalysts

R.J.H. Grisel, B.E. Nieuwenhuys*

Department of Heterogeneous Catalysis and Surface Chemistry, Gorlaeus Laboratoria, Leiden Institute of Chemistry, PO Box 9502, 2300 RA Leiden, Netherlands

Abstract

The activity of Au/Al_2O_3 and $Au/MO_x/Al_2O_3$ (M = Cr, Mn, Fe, Co, Ni, Cu, and Zn) in low temperature CO oxidation and the oxidation of CH_4 was studied. Generally, addition of MO_x to Au/Al_2O_3 stabilizes small Au particles initially present on the support in heat treatments up to 700°C. All multi-component catalysts show a remarkable enhancement in low temperature CO oxidation compared to the mono-component catalysts. The observed activities are directly related to the average Au particle size, whereas the identity of MO_x is less important. The CH_4 oxidation activity of Au/Al_2O_3 is improved upon addition of MnO_x, FeO_x, CoO_x, and to a lesser extent NiO_x. Measured activities in CH_4 oxidation over $Au/MO_x/Al_2O_3$ decrease in the following order: $CuO_x > MnO_x > CrO_x > FeO_x > CoO_x > NiO_x > ZnO_x$. The high activity observed for CuO_x and CrO_x containing catalysts is assigned to the intrinsically high CH_4 oxidation capability of these oxides themselves. For $Au/MnO_x/Al_2O_3$ a lower apparent activation energy was found than for Au/Al_2O_3 and MnO_x/Al_2O_3, which might point to a promoting effect of MnO_x on Au in the oxidation of CH_4. The results presented support a similar model for both CO and CH_4 oxidation. In this model the reaction takes place at the Au/MO_x perimeter, which is defined as the boundary between Au, MO_x and the gas phase. The reductant, CO or CH_4, is adsorbed on Au, and MO_x is the supplier of O.

Keywords: CO; CH_4; Oxidation; Gold; Metal oxides; Alumina; Promoter effect; Catalyst stability

1. Introduction

Over the past few years supported gold catalysts gained in interest because of a surprisingly high catalytic activity in various reactions [1]. Amongst them, the one that most catches the eye is low temperature CO oxidation [2–19]. Au/TiO_2 [2–11] and Au/Fe_2O_3 [2,12–15] were found capable of oxidizing CO already at room temperature. Although it is generally accepted that the high catalytic activity of supported gold catalysts in low temperature CO oxidation can be accredited to the presence of small gold crystallites, which are stabilized by the support [2,4,10–13,16,17], the nature of the active species remains under discussion. While some authors believe ionic gold provides the active sites for CO oxidation [15,18,19], others claim metallic gold to be the active species [2,10–12]. However, according to many papers the gold/support interface plays an important role [3,6,8,10,16,20].

The good performance of gold-based catalysts in CO oxidation inspired scientists to test these catalysts in other oxidation reactions, such as the epoxidation of alkenes [21–23], oxidative destruction of hydrochlorides [24], and oxidation of CH_4 [25,26].

Waters et al. [26] examined coprecipitated Au on several metal oxides for CH_4 oxidation. The observed

* Corresponding author. Tel.: +71-5274-545; fax: +71-5274-451.
E-mail address: nieuwe_b@chem.leidenuniv.nl (B.E. Nieuwenhuys).

0920-5861/01/$ – see front matter
PII: S0920-5861(00)00510-1

order in activity was $Au/Co_3O_4 > Au/NiO_x > Au/MnO_x > Au/Fe_2O_3 > Au/CeO_x$. CH_4 conversion was found over the most active catalyst, viz. Au/Co_3O_4, already at 250°C. It was suggested that oxidized Au species were needed to obtain CH_4 oxidation at low temperatures, whereas the support contributed to the measured activity at higher temperatures. However, no attention was given to a possible correlation between the average gold particle size and the observed activities. Recent results obtained in our laboratory, however, clearly indicate the existence of such a relation [27].

It is generally known that addition of metal oxides can change the catalytic properties of a platinum group metal catalyst, altering the catalyst's activity, selectivity, or stability. For example, the oxidation of CO over noble metal catalysts can be improved by addition of MnO_x [28,29], CoO_x [28–31], LaO_x [31], and CeO_x [32]. MnO_x was also reported to enhance the reduction of NO by CO over Pt/SiO_2 [29], Pd/SiO_2 [33] and reduction of NO with propene over Au/Al_2O_3 [34]. Addition of metal oxides was also reported to alter the catalytic activity in hydrocarbon oxidation. For example, the hydrocarbon oxidation activity of Pd/Al_2O_3 can be improved by addition of alkaline earth metals, such as Mg, Ca, Sr, and Ba, whereas addition of alkaline metals (Na, K) was found to have a negative effect on the catalyst performance [35]. Furthermore, CH_4 oxidation over Pd/Al_2O_3 was found to proceed more swiftly when CrO_x [36] or MnO_x [37] was added.

The work presented in this paper deals with a comparative study of the oxidation of CO and CH_4 over gold supported on alumina. The influence of addition of first row transition metal oxides on the average gold crystallite size and the oxidation activity is studied. Possible models for CO and CH_4 oxidation over Au based catalysts are discussed.

2. Experimental

2.1. Catalyst preparation

Generally, the catalytic activity of Au based catalysts strongly depends on the presence of small Au clusters. In order to obtain similar Au loading and dispersion on all catalysts first a standard 5 wt.% Au/Al_2O_3 was prepared by homogeneous deposition precipitation (HDP) using urea as precipitating agent [38]. For that purpose, the accurate amount of $HAuCl_4$ (Aldrich, 99.999%) was dissolved in demineralized water and added to γ-Al_2O_3 (Engelhard, code: Al-4172 P). The pH of the solution was about 4. Excess urea (Acros, p.a.) was added. The suspension was vigorously stirred and heated to 70–75°C in order to decompose the urea. This temperature was maintained until the pH of the solution reached 8. The suspension was then cooled down and filtered. The resulting Au/Al_2O_3 was dried overnight at 80°C in air and subsequently reduced in a flow of H_2 up to 300°C (heating rate, 5°C min^{-1}). The catalyst was kept at 300°C for 30 min (standard Au/Al_2O_3), cooled down and stored under ambient conditions. Part of the standard catalyst was calcined in a flow of O_2 at 400°C with a heating rate of 5°C min^{-1} and kept at this temperature for 30 min (calcined Au/Al_2O_3).

A selection of transition metal oxides (MO_x) were applied to the standard catalyst by the same method with an intended Au:M atomic ratio of 1 (M = Cr, Mn, Fe, Co, Ni, Zn). The samples were dried at 80°C in air for at least 16 h followed by calcination in a flow of O_2 at 400°C (heating rate, 5°C min^{-1}). The catalysts were kept at 400°C for 30 min. For a proper mutual comparison of the 'promoted' Au catalysts also the corresponding MO_x/Al_2O_3 catalysts were prepared as described above.

2.2. Characterization methods

X-ray diffraction (XRD) measurements were performed using a Philips Goniometer PW 1050/25 diffractometer equipped with a PW Cu 2103/00 X-ray tube operating at 50 kV and 40 mA. From the observed XRD line broadening the average Au crystallite size was calculated by using the simple Scherrer equation [39].

The effect of calcination on the average Au particle size and particle size distribution of Au/Al_2O_3 and $Au/MnO_x/Al_2O_3$ was examined in more detail with transmission electron microscopy (TEM). TEM experiments were performed using a Philips CM 30 T microscope. The energy of the used electrons was 300 kV. Samples were mounted on a micro-grid carbon polymer supported on a copper grid by placing a few droplets of a suspension of ground sample in ethanol on the grid, followed by drying at ambient

conditions. Elemental analysis was performed using a LINK EDX system. From each catalyst about 300 Au particles were measured in order to obtain a good statistical particle size distribution.

The Au loading was determined by atomic absorption spectroscopy (AAS) using a Perkin Elmer 3100 with an air/acetylene flame. For that purpose, the catalysts were dissolved in hot aqua regia. Then the solution was cooled down and diluted with demineralized water before performing analysis.

2.3. Activity measurements

The oxidation reactions were carried out in a lab-scale fixed-bed reactor. Prior to measurement, the catalysts were reduced in 4 vol.% H_2 balanced in He at 300°C (heating rate, 10°C min^{-1}) and kept at 300°C for 30 min. The reactor was cooled down under a flow of He before introducing the reactant flow. The reactant flow (30 ml min^{-1}) consisted of 2.0 vol.% CO and 2.0 vol.% O_2 in He for CO oxidation, and 0.8 vol.% CH_4 and 3.2 vol.% O_2 in He for CH_4 oxidation experiments. After stabilization at room temperature for 30 min two reaction cycles of one heating and one cooling curve were recorded consecutively to monitor possible hysteresis and catalyst deactivation. On-line gas analysis was performed using a VG quadruple MS (model 560), and a Chrompack CP9001 gas chromatograph equipped with a Hayesep N column and flame ionization detector.

To diminish effects of variations in CO or CH_4 oxidation activity during reaction due to sintering, morphology changes, or changes in oxidation state of the applied MO_x, the second heating curve was used for mutual comparison of the different catalysts.

3. Results

3.1. Catalyst characterization

Fresh Au/Al_2O_3, before and after calcination, was characterized by XRD, TEM, and AAS. The Au loading was found to be 5.1 wt.%, which indicates a complete deposition of Au onto the support. This is not always the case when using different deposition methods [19,27]. Characterization by XRD and TEM indicated the presence of Au particles with an average diameter of 3.6 ± 1.4 nm for the uncalcined catalyst and 9.2 ± 3.4 nm for the catalyst calcined in O_2 at 400°C. Elemental analysis of both these catalysts did not indicate the presence of any residual Cl^- or other contaminants.

Fig. 1 shows the XRD patterns of fresh Au/Al_2O_3 and $Au/MO_x/Al_2O_3$ after background subtraction for the support. It is clear that addition of MO_x to Au/Al_2O_3 followed by calcination at 400°C caused

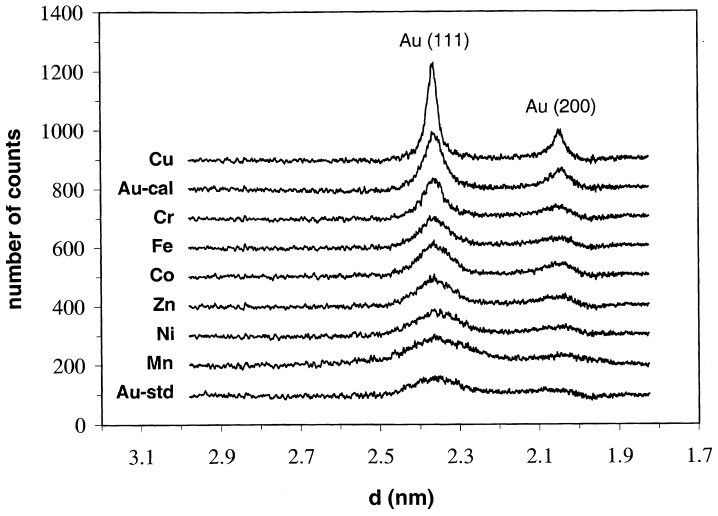

Fig. 1. XRD patterns of standard Au/Al_2O_3 (Au-std), Au/Al_2O_3 after calcination at 400°C (Au-cal), and $Au/MO_x/Al_2O_3$ after calcination at 400°C (M = Cr, Mn, Fe, Co, Ni, Cu, and Zn).

Table 1
Average Au particle sizes (nm) of $Au/MO_x/Al_2O_3$ from XRD line broadening

Addition	Au/Al_2O_3[a]	Standard catalyst[b]	Cr	Mn	Fe	Co	Ni	Cu	Zn
Fresh catalyst	2.7	9.8	9.6	3.7	6.7	6.0	4.0	18.2	5.3
After CO oxidation	3.9	9.0	9.1	3.9	6.9	6.2	4.3	18.7	5.2
After CH_4 oxidation	11.0	12.0	10.6	4.3	6.8	6.3	4.8	19.5	5.7

[a] After reduction in pure H_2 for 30 min at 300°C (Au-std).
[b] After calcination in O_2 for 30 min at 400°C (Au-cal).

sintering of the Au particles. The sintering behavior was found to depend strongly on the identity of the added MO_x, where as addition of MnO_x did not change the average particle size much (3.7 nm), addition of CuO_x resulted in huge Au agglomerates (18.2 nm). No diffraction peaks of MO_x were observed. The average Au particle sizes, as determined from XRD line broadening, are given in Table 1.

The Au crystallites on the standard catalyst were found to sinter at a calcination temperature of 400°C. This is in agreement with literature, where sintering of supported Au particles was reported in both oxidative and reductive environment at temperatures above 400°C [6,9,19]. Low temperature CO oxidation (300°C) did not change the average Au crystallite size significantly. However, the high temperatures needed for CH_4 oxidation (700°C) did induce a clear Au particle growth.

Generally, addition of MO_x to Au/Al_2O_3 seemed to stabilize the initially small average Au particles during calcination at 400°C to a certain extent. Only for the CrO_x and CuO_x containing catalysts a considerable larger Au particle size was observed (Table 1). This behavior was confirmed with TEM experiments on $Au/MnO_x/Al_2O_3$. Small Au particles initially present on the standard catalyst (Fig. 2a) sintered considerably during the calcination procedure, whereas addition of MnO_x inhibited Au particle growth to a large extent (Fig. 2b). For MnO_x itself a rather homogeneous dispersion was found. Under the relatively mild reaction conditions for CO oxidation no further sintering was observed. Surprisingly, however, was the perception that added MO_x also inhibited Au particle growth at the high temperatures needed for CH_4 oxidation.

3.2. CO oxidation

MO_x/Al_2O_3 catalysts were found not to be particularly active in low temperature CO oxidation. No significant CO conversion was detected below 150°C for all these catalysts, and full conversion was only reached over CoO_x/Al_2O_3 in the temperature range studied (up to 350°C). CO oxidation over standard Au/Al_2O_3 proceeded smoothly, as can be expected from literature data [40]. Full conversion over Au/Al_2O_3 was already reached at 160°C. After calcination at 400°C, Au/Al_2O_3 was found to have lost some of its activity. Since small Au particles (1–6 nm) are beneficial for low temperature CO oxidation [1,4,6,10,13], the observed decrease in activity is probably due to sintering of the Au crystallites as noted in Table 1.

Addition of MO_x to Au/Al_2O_3 generally increased the activity of the catalyst. Fig. 3 gives an example of the enhancement in activity induced by addition of MO_x. Shown are the second heating curves for CO oxidation over standard Au/Al_2O_3 (Au-std), calcined Au/Al_2O_3 (Au-cal), MnO_x/Al_2O_3, and $Au/MnO_x/Al_2O_3$. It was found that addition of MnO_x enhanced the catalyst performance in low temperature CO oxidation enormously. Next to MnO_x, also addition of NiO_x and ZnO_x, and to a lesser extent FeO_x and CoO_x, were found to enhance the catalytic oxidation of CO over Au/Al_2O_3 (Table 2). The activity in CO oxidation over $Au/MO_x/Al_2O_3$ drops in the following order: $MnO_x > NiO_x > ZnO_x > FeO_x > CoO_x > CrO_x > CuO_x$. After the first heating curve a slight decrease in activity was found for all $Au/MO_x/Al_2O_3$. No clear indication of hysteresis was found.

3.3. CH_4 oxidation

Two consecutive reaction cycles of CH_4 oxidation activity over standard Au/Al_2O_3 (Au-std) are shown in Fig. 4. After the first heating curve the catalyst was found to deactivate to a certain extent. This deactivation was probably due to sintering of the Au

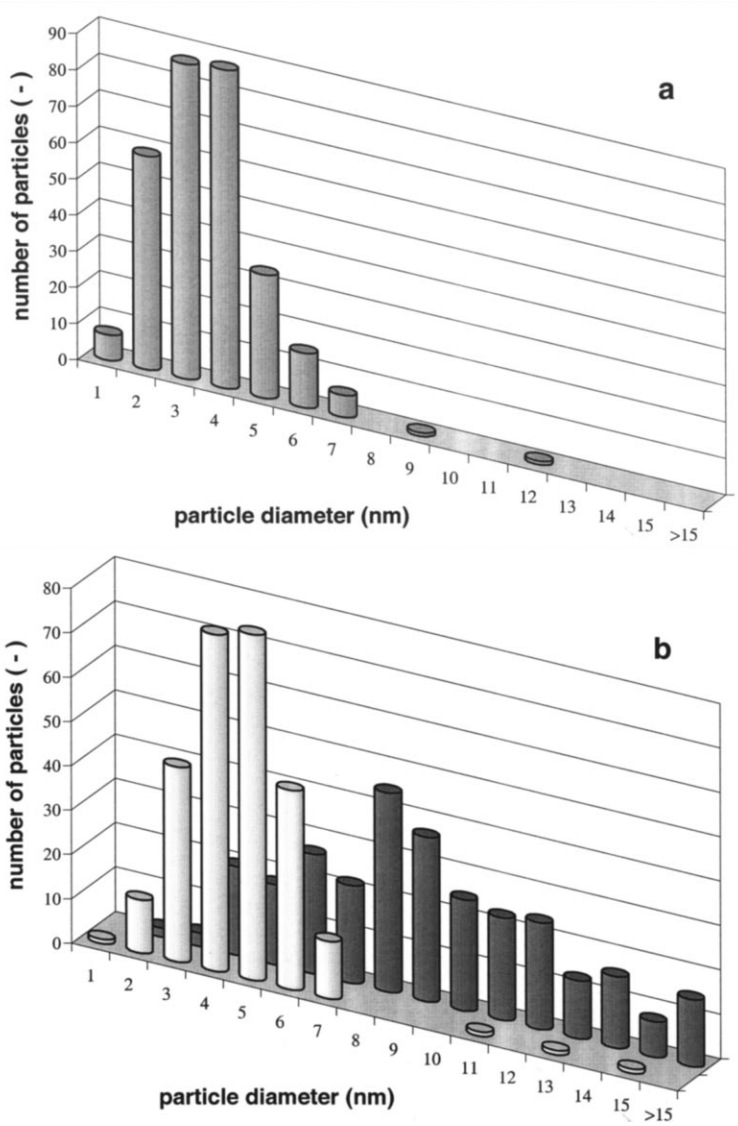

Fig. 2. Size distribution of Au particles supported on Al_2O_3: (a) before calcination; (b) after calcination in O_2 at 400°C for 30 min, with Mn (light bars) and without Mn (dark bars) addition.

particles during the first heating stage of the reaction (Table 1). Consecutive cooling and heating curves did not result in any further significant deactivation of the catalyst. To minimize variations in CH_4 oxidation activity due to catalyst deactivation, the second heating curve was used to compare the different catalysts.

The data were fit to a sigmoidal function of the following form:

$$\alpha = b[1 - \exp\{-(k(T - c))^d\}] \quad (1)$$

in which α is the fraction of CH_4 consumed, T the temperature (°C), and b, k, c, and d are constants. The constants were varied until the best fit was found. The

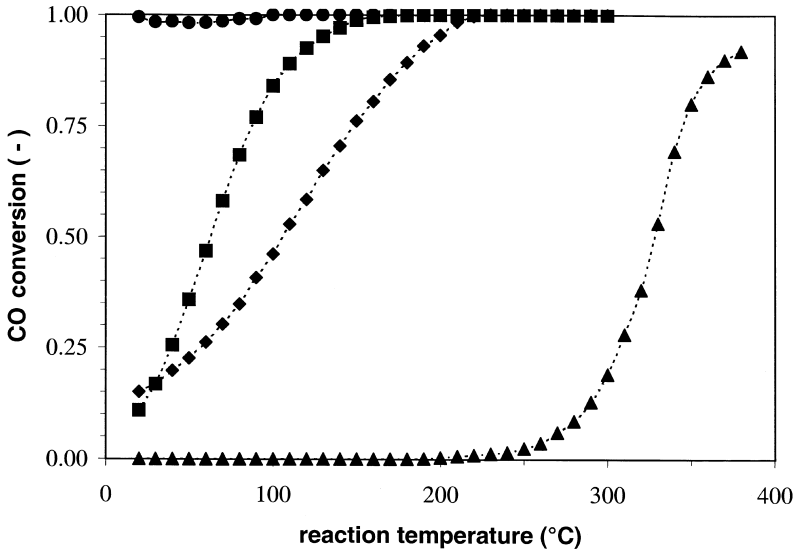

Fig. 3. CO conversion versus temperature ($CO:O_2 = 1:1$) over standard Au/Al_2O_3 (■), Au/Al_2O_3 calcined at 400°C (◆), MnO_x/Al_2O_3 (▲), and $Au/MnO_x/Al_2O_3$ (●).

derivative of (1), $d\alpha/dT$, corresponds to the change in conversion over a temperature interval dT, and thus is characteristic of the maximum rate of reaction. The temperature of the maximum of $d\alpha/dT$ provides a good parameter to express the catalyst activity. Therefore it was chosen to facilitate mutual comparison of CH_4 oxidation activities of the different catalysts, and will further be denoted as $(d\alpha/dT)_{max}$. The values for $(d\alpha/dT)_{max}$ are summarized in Table 3.

$(d\alpha/dT)_{max}$ values indicate that from the studied MO_x/Al_2O_3 only CrO_x/Al_2O_3, and CuO_x/Al_2O_3 were more than moderately active, pointing out the good hydrocarbon oxidation capability of these oxides [41–43]. NiO_x/Al_2O_3 and ZnO_x/Al_2O_3 were the least active in CH_4 oxidation. Instead, detectable amounts of CO were observed in the high temperature region (>500°C), which indicates a non-complete oxidation of CH_4 over these catalysts. The CH_4 oxidation activities of MO_x/Al_2O_3 fall in the following order: $CuO_x > CrO_x > FeO_x > MnO_x > CoO_x > NiO_x > ZnO_x$. Au/Al_2O_3 was found to be slightly more active than FeO_x/Al_2O_3, but considerably

Table 2
The CO oxidation activity of Au/Al_2O_3 and $Au/MO_x/Al_2O_3$

Catalyst MO_x/Al_2O_3	Conversion α (300°C)	Catalyst $Au/MO_x/Al_2O_3$	Conversion α (25°C)	$T_{99\%}$ (°C)
		Au/Al_2O_3[a]	0.11	151
Al_2O_3	<0.01	Au/Al_2O_3[b]	0.15	213
CrO_x/Al_2O_3	0.04	$CrO_x/Au/Al_2O_3$	0.12	191
MnO_x/Al_2O_3	0.19	$MnO_x/Au/Al_2O_3$	1.00	<25
FeO_x/Al_2O_3	0.43	$FeO_x/Au/Al_2O_3$	0.50	100
CoO_x/Al_2O_3	0.62	$CoO_x/Au/Al_2O_3$	0.40	114
NiO_x/Al_2O_3	0.12	$NiO_x/Au/Al_2O_3$	0.41	77
CuO_x/Al_2O_3	0.35	$CuO_x/Au/Al_2O_3$	0.18	144
ZnO_x/Al_2O_3	0.01	$ZnO_x/Au/Al_2O_3$	0.29	88

[a] Au/Al_2O_3 after reduction in pure H_2 for 30 min at 300°C (Au-std).
[b] Standard catalyst after calcination in O_2 for 30 min at 400°C (Au-cal).

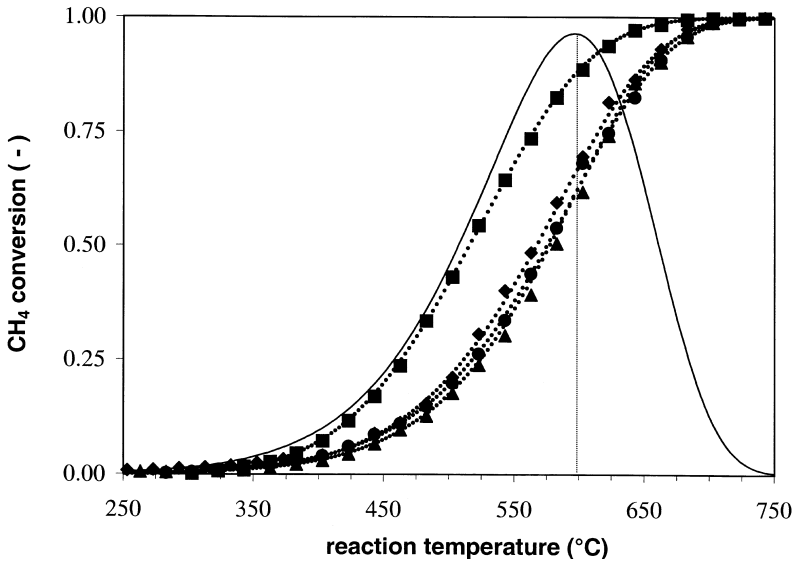

Fig. 4. CH_4 oxidation activity over standard Au/Al_2O_3 (CH_4:O_2 = 1:4). First heating stage (■), first cooling stage (◆), second heating stage (▲), and second cooling stage (●). Sigmoidal fits (···), derivative of second heating stage (—).

less active than CuO_x/Al_2O_3 and CrO_x/Al_2O_3. MO_x/Al_2O_3 were found to be rather stable under the reaction conditions used, i.e. no significant deactivation was observed after the first heating curve.

Fig. 5 illustrates the change in CH_4 oxidation activity of Au/Al_2O_3 upon MO_x addition. Adding NiO_x and ZnO_x to Au/Al_2O_3 did not change the activity much. However, similar to CH_4 oxidation over NiO_x/Al_2O_3 and ZnO_x/Al_2O_3 some CO was detected in the high temperature range (>500°C), indicating incomplete oxidation of CH_4 also over these catalysts. CoO_x addition only slightly improved the catalyst's performance, whereas addition of CrO_x, MnO_x, FeO_x, and CuO_x resulted in catalysts with a significantly higher CH_4 oxidation activity. Albeit the large catalyst improvement due to addition of CrO_x and CuO_x can easily be understood by assuming high activity in CH_4 oxidation of the applied MO_x itself

Table 3
Catalytic oxidation of CH_4 over Au/Al_2O_3 and $Au/MO_x/Al_2O_3$

Catalyst Mo_x/Al_2O_3	E_a (kJ mol^{-1})	$(d\alpha/dT)_{max}$ (°C)	Catalyst $MO_x/Au/Al_2O_3$	E_a (kJ mol^{-1})	$(d\alpha/dT)_{max}$ (°C)
			Au/Al_2O_3[a]	71	597
Al_2O_3[b]	140	–[c]	Au/Al_2O_3[d]	71	601
CrO_x/Al_2O_3	131	558	$CrO_x/Au/Al_2O_3$	96	550
MnO_x/Al_2O_3	103	610	$MnO_x/Au/Al_2O_3$	63	520
FeO_x/Al_2O_3	108	604	$FeO_x/Au/Al_2O_3$	70	562
CoO_x/Al_2O_3	116	657	$CoO_x/Au/Al_2O_3$	73	577
NiO_x/Al_2O_3[b]	116	674	$NiO_x/Au/Al_2O_3$[b]	73	584
CuO_x/Al_2O_3	95	512	$CuO_x/Au/Al_2O_3$	103	504
ZnO_x/Al_2O_3[b]	135	695	$ZnO_x/Au/Al_2O_3$[b]	70	600

[a] Au/Al_2O_3 after reduction in pure H_2 for 30 min at 300°C (Au-std).
[b] Detectable amounts of CO observed (see text).
[c] Conversion stays below 0.50 in the temperature range studied.
[d] Standard catalyst after calcination in O_2 for 30 min at 400°C (Au-cal).

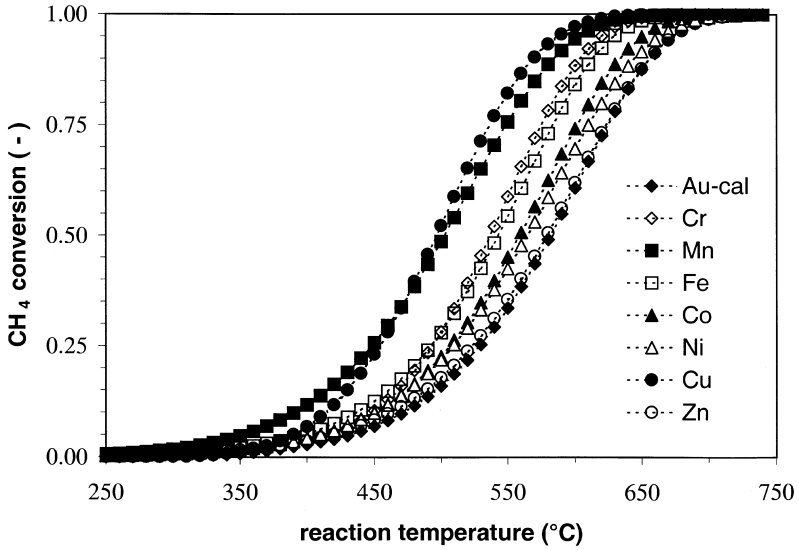

Fig. 5. CH_4 conversion versus temperature (°C) over Au/Al_2O_3 calcined at 400°C (Au-cal) and $Au/MO_x/Al_2O_3$ (M = Cr, Mn, Fe, Co, Ni, Cu, and Zn); sigmoidal fits (···).

[41–43], the improvement due to MnO_x and FeO_x addition is less obvious. The CH_4 oxidation activities over Au-containing $Au/MO_x/Al_2O_3$ was found to obey the following order: $CuO_x > MnO_x > CrO_x > FeO_x > CoO_x > NiO_x > ZnO_x$. An interesting and important feature was that, unlike Au/Al_2O_3, $Au/MO_x/Al_2O_3$ were found stable with regard to deactivation under the severe reaction conditions.

The apparent activation energies for CH_4 oxidation were calculated from the temperature dependency of

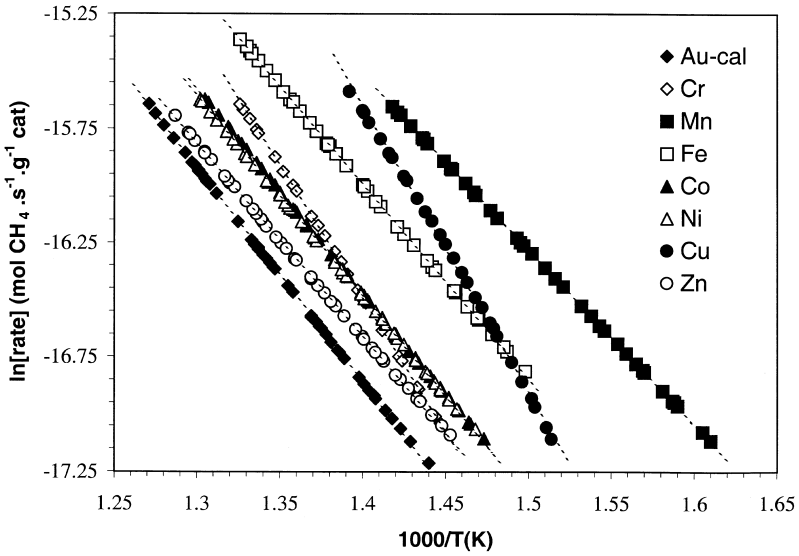

Fig. 6. Arrhenius plots for CH_4 oxidation versus the reciprocal temperature (K) over Au/Al_2O_3 calcined at 400°C (Au-cal) and $Au/MO_x/Al_2O_3$ (M = Cr, Mn, Fe, Co, Ni, Cu, and Zn).

the reaction rate at low conversions ($0.05 < \alpha < 0.20$). The Arrhenius plots of CH_4 oxidation over Au/Al_2O_3 and $Au/MO_x/Al_2O_3$ are shown in Fig. 6. The apparent activation energies (E_a) are summarized in Table 3. Considering the values obtained for E_a, $Au/MO_x/Al_2O_3$ catalysts can roughly be divided into two groups. A large group with similar E_a as Au/Al_2O_3 (M = Mn, Fe, Co, Ni, and Zn), and a smaller group with significantly higher E_a (M = Cr and Cu).

4. Discussion

It is generally accepted that small Au particles are beneficial for both low temperature CO oxidation [1,4,6,10,13] and CH_4 oxidation [27]. This is attributed to either the presence of a large total Au/support interface [3,6,8,10,16,20] or the presence of special sites such as coordinately unsaturated Au surface atoms [7,44], a special electronic structure of very small Au particles [45], or ionic Au species [15,18,19,26] particularly present on small Au particles. Both a large interface and the possible presence of special sites are relatively more abundant when dealing with small Au particles, leaving it very difficult to specify the actual active Au species.

When assuming that the Au particles are hemispherical, uniform in size, and no Au atoms migrate into the oxide lattice of the support during reaction or disappear otherwise, the total Au surface area can be written as follows:

$$A_{tot} = \frac{6V_{tot}}{d_{Au}} \quad (2)$$

in which A_{tot} represents the total Au surface area, V_{tot} the total volume of the Au particles, which is constant in this consideration, and d_{Au} the Au particle size. In like manner, the total Au/MO_x perimeter, P_{tot}, can be written as follows:

$$P_{tot} = \frac{12V_{tot}}{d_{Au}^2} \quad (3)$$

The Au/MO_x perimeter is defined as boundary between Au, MO_x (including support), and the gas phase. Eq. (3) implies that the total perimeter decreases exponentially with an increase of the particle diameter. Therefore, small particles suffer disproportionately from sintering than large particles. For instance, the total perimeter accompanied by a change in particle size from 1 to 2 nm decreases with the same factor as a change in particle size from 10 to 20 nm. Thus, when comparing supported Au catalysts it is very important to consider slight discrepancies in particle size, especially when dealing with particles smaller than 5 nm. Unfortunately, the preparation of $Au/MO_x/Al_2O_3$ out of a standard Au/Al_2O_3 catalyst with a well-defined particle size and particle size distribution did not result in catalysts with similar Au particle sizes. Therefore, the results presented above should be considered with care. The alteration in particle size may originate from redistribution of Au in solution during MO_x deposition, or during calcination.

Small Au particles tend to sinter during heat treatments above 400°C [6,9,19]. This is also illustrated in this paper. After calcination of Au/Al_2O_3 the average Au particle size increased by a factor 3.5 (Table 1). Sintering of small Au particles can be inhibited upon addition of MO_x, even at temperatures as high as 700°C, which were used in CH_4 oxidation reactions. Although the background of this stabilizing effect is still unclear, it was found to depend strongly on the identity of the applied MO_x. Kang and Wan [46] already noticed such a stabilizing effect for Au/zeolite-Y upon addition of FeO_x.

Apparently, addition of transition metal oxides to Au/Al_2O_3 can improve the catalytic activity in both low temperature CO oxidation and to a lesser extent CH_4 oxidation. However, the origin of this improvement seems to be different for both reactions. Fig. 7a shows the $T_{99\%}$ and $(d\alpha/dT)_{max}$ values for, respectively, CO and CH_4 oxidation as function of the average Au particle diameter as determined from XRD line broadening. For low temperature CO oxidation over $Au/MO_x/Al_2O_3$ there is clearly a relationship between activity and average Au particle size. Outside of experimental errors, the deviation of these points from the drawn line can probably be related to the assumptions made about the particles themselves. As seen in TEM the particles do have a definite size distribution (Fig. 2a and b) and it is also not apparent that all particles are hemispherical. Moreover, although incorporation of Au into the oxide lattice is not very probable, parts of Au may be covered by MO_x patches, reduc-

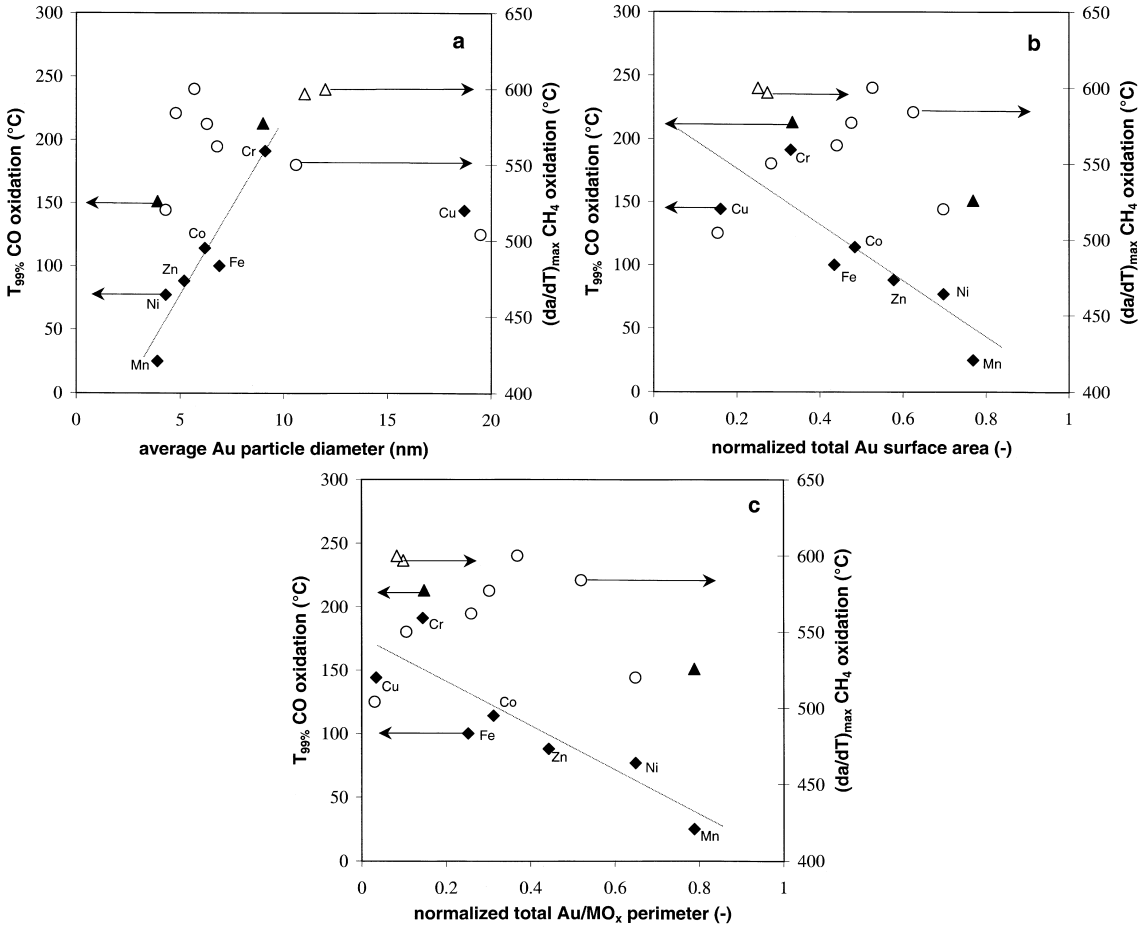

Fig. 7. $T_{99\%}$ for CO oxidation over Au/Al_2O_3 (▲) and $Au/MO_x/Al_2O_3$ (◆): (a) versus the average Au particle size, right axis: $(d\alpha/dT)_{max}$ for CH_4 oxidation over Au/Al_2O_3 (△) and $Au/MO_x/Al_2O_3$ (○) versus the average Au particle size; (b) versus the total calculated Au surface area, right axis: $(d\alpha/dT)_{max}$ for CH_4 oxidation over Au/Al_2O_3 (△) and $Au/MO_x/Al_2O_3$ (○); (c) versus the total calculated Au/MO_x perimeter, right axis: $(d\alpha/dT)_{max}$ for CH_4 oxidation over Au/Al_2O_3 (△) and $Au/MO_x/Al_2O_3$ (○).

ing the amount of surface Au active in low temperature CO oxidation. Adding MO_x did improve the CO oxidation activity more than can be expected from the presence of stable small Au particles alone, however, the nature of MO_x did not seem to be very important (Table 2). In contrast with CO oxidation, no direct correlation is observed between the CH_4 oxidation activity and average Au particle size. The observed activity varies with the nature of the applied oxide (Table 3). However, since previous results [27] show that the Au particle size does in fact influence the CH_4 oxidation activity considerably, one can conclude that the CH_4 oxidation activity over $Au/MO_x/Al_2O_3$ both depends on the Au particle size and the identity of the added oxide.

In order to determine the true identity of the active Au species the $T_{99\%}$ and $(d\alpha/dT)_{max}$ values are also plotted as function of the calculated total Au surface area (Fig. 7b) and the total Au/MO_x perimeter (Fig. 7c). Unfortunately, on the basis of our present results no real distinction between the importance of a large Au surface area and a large Au/MO_x perimeter can be made. A more detailed study on the Au particle size, particle size distribution and shape of the

particles might lead to a better understanding of this problem.

4.1. Model for CO oxidation over $Au/MO_x/Al_2O_3$

The CO oxidation activity of the studied catalysts were compared at high conversion. Under these conditions the presence of mass and heat transfer limitations is evident. Because of the high activity of Au-containing catalysts already at room temperature (Table 2), no kinetic data could be collected under differential conditions. Therefore, nothing can be said about the intrinsic catalytic activity, and thus the true kinetic behavior of these catalysts in low temperature CO oxidation. However, it is clear that the rate of low temperature CO oxidation over Au/Al_2O_3 can be enhanced by addition of suitable MO_x. Since none of the selected MO_x was found to be active in the low temperature region (<150°C), the enhancement is probably due to either changes in the Au phase or synergistic effects between Au and the applied MO_x. Mergler et al. [30] discussed a number of models, which could account for the observed improvement in CO oxidation activity over Pt/SiO_2 upon addition of CoO_x. Some models imply that the CO inhibition, which is typical of Pt-only catalysts at low temperatures [20,47], is diminished because of a lower heat of CO adsorption on Pt in the presence of CoO_x, by a 'promoting' effect of CoO_x or by Co–Pt alloy formation. Since CO only weakly adsorbs on Au and no CO inhibition is expected, these models are not considered any further. Another model is based on the assumption that Co cations can promote the dissociative adsorption of O_2 on Pt by an increased back-donation of electrons into the antibonding orbitals of O_2 adsorbed on Pt. Au, however, is not known to be an effective metal for dissociative adsorption in general. It might be that special Au sites, in particular present on small Au particles, are able to dissociate O_2. For example, Boccuzzi et al. [18] reported an apparent scrambling reaction between CO and O_2 which occurred over Au/ZnO already at room temperature, suggesting that both molecules are activated on Au sites. A recent paper by Liu et al. [48], however, indicated that O_2 does not dissociate on $Au/Fe(OH)_3$, and that oxygen vacancies at the oxide surface adjacent to the Au particles are necessary to obtain any reactivity in low temperature CO oxidation. Actually, AuO_x can be formed from Au and O_2 and the first step must be the dissociative adsorption of O_2. However, in view of the low sticking probability of O_2, accompanied by very low oxidation reaction rates on Au, this model is not very likely. Two other models ascribe the improved activity to a reaction between activated O supplied by CoO_x and CO adsorbed at the Pt/CoO_x interface or on Pt.

From the results obtained for low temperature CO oxidation over $Au/MO_x/Al_2O_3$ (Table 2) it is clear that addition of MO_x generally enhances the activity. The observed activity is directly correlated with the average Au particle size (Fig. 7a). Since addition of MO_x stabilizes the average Au particle size, close contact between Au and MO_x is expected. Therefore, we propose that the reaction takes place between CO adsorbed on Au or at the Au/MO_x perimeter and O donated by MO_x. When CO is adsorbed at or near the Au/MO_x perimeter, no migration of O and CO is necessary. This makes the perimeter an extremely suited spot for reaction to take place.

It was noted that the $Au/MO_x/Al_2O_3$ deactivates to some extent during the first heating curve. During the start of the first heating curve, the applied MO_x is still partially reduced due to the reductive pretreatment prior to measurement. The oxygen vacancies present on MO_x can be filled with O_2 from the feed already at room temperature leaving activated O on the surface. This highly reactive O immediately reacts with adsorbed CO giving CO_2, which leaves the surface. However, this O-removal can be slower than O_2 supply. When all oxygen vacancies are filled, i.e. when MO_x is completely reoxidized, another mechanism should account for the supply of active O. One possible model is that CO at the Au/MO_x perimeter reacts with O from the oxide lattice, leaving an oxygen vacancy. O_2 from the feed fills up the oxygen vacancy as described above. This so-called Mars–van Krevelen mechanism is well known for transition metal oxides in redox reactions [49,50]. Subtraction of O out of the lattice requires a certain E_a, and therefore will occur only at slightly elevated temperatures. This could account for the slight deactivation observed after the first heating curve for CO oxidation over prereduced $Au/MO_x/Al_2O_3$.

4.2. Model for CH_4 oxidation over $Au/MO_x/Al_2O_3$

Generally, the difficult step in CH_4 oxidation is considered to be C–H bond activation. Bare Al_2O_3 has little activity in CH_4 oxidation. The E_a was measured to be about 140 kJ mol^{-1} (Table 3). Upon deposition of Au the E_a decreased by a factor 2. Regarding the large decrease in E_a after addition of Au, the role of Au is probably activation of CH_4. Active O, needed for reaction, might originate from dissociative adsorption of O_2 near the Au/Al_2O_3 perimeter or dehydroxylation of the Al_2O_3 surface [51,52]. The activity of Au/Al_2O_3 was found to depend on the average Au particle size [27]. This is consistent with a model in which CH_4 is dissociatively adsorbed on Au or the Au/Al_2O_3 perimeter and reacts with O also present at the perimeter due to surface reactions on Al_2O_3 at elevated temperatures.

Upon addition of MO_x the measured activity did not correlate with the average Au particle size, as is the case for low temperature CO oxidation (Fig. 7a). The nature of MO_x was found to be important. Generally, MO_x with higher intrinsic activity (M = Cu, Cr, Fe, Mn, Co) improved the catalyst more than less active oxides (M = Ni, Zn). The observed E_a (Table 3) could roughly be divided into three groups. Adding FeO_x, CoO_x, NiO_x, and ZnO_x to Au/Al_2O_3 did not change E_a, indicating a similar reaction mechanism over these catalysts. The improved activity measured for FeO_x, CoO_x, and NiO_x can be understood when assuming that addition of these oxides creates more sites, which are capable of supplying active O, via, e.g. a Mars–van Krevelen mechanism [49,50].

$Au/MnO_x/Al_2O_3$ was found to have a slightly lower E_a. Assuming C–H bond activation is still the rate determining step, it must be concluded that MnO_x can modify the Au particles in such a way that CH_4 activation is facilitated. The role of MnO_x may be twofold. On the one hand it facilitates activation of CH_4 on Au, and on the other hand it is also the supplier of active O. CH_4 activation on MnO_x itself is not likely to be very important regarding the high E_a for CH_4 oxidation over MnO_x/Al_2O_3 (Table 3).

The E_a found for $Au/CuO_x/Al_2O_3$ and $Au/CrO_x/Al_2O_3$ was considerably larger than that of the other multi-component catalysts. The E_a of $Au/CuO_x/Al_2O_3$ was similar to that of CuO_x/Al_2O_3. This might indicate that Au is inactive in this catalyst at low conversions, and that the measured activity is from CuO_x alone. At higher temperatures a dual-site character as proposed by Waters et al. [26] may be considered. For $Au/CrO_x/Al_2O_3$ a dual-site character is more evident. The E_a of this catalyst seems merely to be an average of those of Au/Al_2O_3 and CrO_x/Al_2O_3, where as E_a does vary, $(d\alpha/dT)_{max}$ of Au containing CrO_x/Al_2O_3 does not change considerably. The existence of this dual-site character may well be explained by a lack of interaction between Au and CrO_x. However, a more detailed study about the interaction of Au and MO_x, in general, is necessary.

5. Conclusions

Apparently, the addition of transition metal oxides to Au/Al_2O_3 can improve the catalytic activity in both low temperature CO oxidation and to a lesser extent CH_4 oxidation. However, the origin of this improvement seems to be different for both reactions. Whereas the catalytic activity of $Au/MO_x/Al_2O_3$ in low temperature CO oxidation merely seems to be correlated with the average Au particle size and the presence of any oxide, the activity in CH_4 oxidation appears to depend on both the Au particle size and the identity of the applied oxide. The measured oxidation activity of CH_4 over $Au/MO_x/Al_2O_3$ decreases in the order: $CuO_x > MnO_x > CrO_x > FeO_x > CoO_x > NiO_x > ZnO_x$.

$Au/MnO_x/Al_2O_3$ is found to be by far the best catalyst for CO oxidation. For CH_4 oxidation the highest activity is observed for CuO_x/Al_2O_3 immediately followed by $Au/MnO_x/Al_2O_3$. Regarding the obtained apparent activation energies for CH_4 oxidation over these catalysts, the active phase of $Au/CuO_x/Al_2O_3$ is more probable to be CuO_x than Au, whereas in $Au/MnO_x/Al_2O_3$ the Au and MnO_x seem to cooperate more closely together.

In case of most of the examined $Au/MO_x/Al_2O_3$ catalysts (M = Mn, Fe, Co, Ni, Zn), the results plead for a single model for both low temperature CO oxidation and CH_4 oxidation over Au-based catalysts. In this model the reaction solely takes place at the Au/MO_x perimeter with the reductant adsorbed on Au and MO_x the supplier of O. When the applied MO_x is more than moderately active in oxidation reactions (M = Cr, Cu) the reaction also partly (CrO_x) or predominantly (CuO_x) takes place on MO_x itself.

Acknowledgements

The authors sincerely wish to thank Dr. P.J. Kooyman of the National Center for High Resolution Electron Microscopy, Delft University of Technology, Delft, the Netherlands, for performing the electron microscopy investigations. This work has been performed under auspices of NIOK, the Netherlands Institute for Catalysis Research, Lab report No. UL 99-2-08.

References

[1] M. Haruta, Catal. Today 36 (1997) 153.
[2] M. Haruta, S. Tsubota, T. Kobayashi, H. Kageyama, M. Genet, B. Delmon, J. Catal. 144 (1993) 175.
[3] G.R. Bamwenda, S. Tsubota, T. Nakamura, M. Haruta, Catal. Lett. 44 (1997) 83.
[4] M. Valden, S. Pak, X. Lai, D.W. Goodman, Catal. Lett. 56 (1998) 7.
[5] N.W. Cant, N.J. Ossipoff, Catal. Today 36 (1997) 125.
[6] S. Tsubota, T. Nakamura, K. Tanaka, M. Haruta, Catal. Lett. 56 (1998) 131.
[7] F. Boccuzzi, G. Cerrato, F. Pinna, G. Strukul, J. Phys. Chem. B 102 (1998) 5733.
[8] J.-D. Grunwaldt, A. Baiker, J. Phys. Chem. B 103 (1999) 1002.
[9] M.A. Bollinger, M.A. Vannice, Appl. Catal. B 8 (1996) 417.
[10] M. Haruta, Catal. Surveys Jpn. 1 (1997) 61.
[11] M.A.P. Dekkers, M.J. Lippits, B.E. Nieuwenhuys, Catal. Lett. 56 (1998) 195.
[12] M. Haruta, N. Yamada, T. Kobayashi, S. Iijima, J. Catal. 115 (1989) 301.
[13] S.K. Tanielyan, R.L. Augustine, Appl. Catal. A 85 (1992) 73.
[14] A.M. Visco, A. Donato, C. Milone, S. Galvano, React. Kinet. Catal. Lett. 61 (1997) 219.
[15] S. Minicò, S. Scirè, A. Visco, S. Galvano, Catal. Lett. 47 (1997) 273.
[16] D. Cunningham, S. Tsubota, N. Kamijo, M. Haruta, Res. Chem. Intermed. 19 (1993) 1.
[17] G. Srinivas, J. Wright, C.C. Bai, R. Cook, Stud. Surf. Sci. Catal. 101 (1996) 427.
[18] F. Boccuzzi, A. Chiorino, S. Tsubota, M. Haruta, Catal. Lett. 29 (1994) 225.
[19] C.-K. Chang, Y.-J. Chen, C.-t. Yeh, Appl. Catal. A 174 (1998) 13.
[20] B.E. Nieuwenhuys, in: R.W. Joyner, R.A. van Santen (Eds.), Elementary Reaction Steps in Heterogeneous Catalysis, Kluwer Academic Publishers, Dordrecht, the Netherlands, 1993.
[21] H. Nakatsuji, Z-.M. Hu, H. Nakai, K. Ikeda, Surf. Sci. 387 (1997) 328.
[22] T.A. Nijhuis, B.J. Huizinga, M. Makkee, J.A. Moulijn, Ind. Eng. Chem. Res. 38 (1999) 884.
[23] T. Hayashi, K. Tanaka, M. Haruta, J. Catal. 178 (1998) 566.
[24] B. Chen, C. Bai, R. Cook, J. Wright, C. Wang, Catal. Today 30 (1996) 15.
[25] K. Blick, T.D. Mitrelias, J.S.J. Hargreaves, G.J. Hutchings, R.W. Joyner, C.J. Kiely, F.E. Wagner, Catal. Lett. 50 (1998) 211.
[26] R.D. Waters, J.J. Weimer, J.E. Smith, Catal. Lett. 30 (1995) 181.
[27] R.J.H. Grisel, B.E. Nieuwenhuys, J. Catal. 191 (2000) 430.
[28] Y.J. Mergler, A. van Aalst, J. van Delft, B.E. Nieuwenhuys, Appl. Catal. B 10 (1996) 245.
[29] Y.J. Mergler, A. van Aalst, J. van Delft, B.E. Nieuwenhuys, Stud. Surf. Sci. Catal. 96 (1995) 163.
[30] Y.J. Mergler, J. Hoebink, B.E. Nieuwenhuys, J. Catal. 167 (1997) 305.
[31] M. Skoglundh, H. Johansson, L. Löwendahl, K. Jansson, L. Dahl, B. Hirschauer, Appl. Catal. B 7 (1996) 299.
[32] Y.-F. Yu-Yao, J.T. Kummer, J. Catal. 106 (1987) 307.
[33] J.F. Trillat, J. Massardier, B. Moraweck, H. Praliaud, A.J. Renouprez, Stud. Surf. Sci. Catal. 116 (1998) 103.
[34] A. Ueda, M. Haruta, Appl. Catal. B 18 (1998) 115.
[35] H. Shinjoh, N. Isomura, H. Sobukawa, M. Sugiura, Stud. Surf. Sci. Catal. 116 (1998) 83.
[36] S. Khairulin, B. Béguin, E. Garbowski, M. Primet, J. Chem. Soc., Faraday Trans. 93 (1997) 2217.
[37] J. Carnö, M. Ferrandon, E. Björnbom, S. Järås, Appl. Catal. A 155 (1997) 265.
[38] J.W. Geus, Dutch Patent Appl. 6705 (1967) 259.
[39] P. Scherrer, Nachr. k. Ges. Wiss, Göttingen, 98 (1918).
[40] M.C. Kung, J.H. Lee, A.C. Kung, H.H. Kung, Stud. Surf. Sci. Catal. 101 (1996) 701.
[41] J.G. McCarty, Y.-f. Chang, V.L. Wong, in: Proceedings of the Symposium on Catalytic Combustion, Div. Petroleum Chem., San Francisco, CA, April 13–17, 1997, p. 158.
[42] G. Busca, M. Daturi, E. Finocchio, V. Lorenzelli, G. Ramis, R.J. Willey, Catal. Today 33 (1997) 239.
[43] R. Rudham, M.K. Sanders, J. Catal. 27 (1972) 287.
[44] M. Ruff, S. Frey, B. Gleich, R.J. Behm, Appl. Phys. A 66 (1998) S513.
[45] M. Valden, X. Lai, D.W. Goodman, Science 281 (1998) 1647.
[46] Y.-M. Kang, B.-Z. Wan, Catal. Today 26 (1995) 59.
[47] S.H. Oh, G.B. Fisher, J.E. Carpenter, D.W. Goodman, J. Catal. 100 (1986) 360.
[48] H. Liu, A.I. Kozlov, A.P. Kozlova, T. Shido, Y. Iwasawa, Phys. Chem., Chem. Phys. 1 (1999) 2851.
[49] C. Kröger, Z. Anorg. Chem. 206 (1932) 289.
[50] P. Mars, D.W. van Krevelen, Chem. Eng. Sci. Spec. Suppl. 3 (1954) 41.
[51] S. Soled, J. Catal. 81 (1983) 252.
[52] A.A. Tsyganenko, P.P. Mardilovich, J. Chem. Soc., Faraday Trans. 92 (1996) 4843.